This is a preproof accepted article for *Mineralogical Magazine*
This version may be subject to change during the production process
DOI: 10.1180/mgm.2025.10141

New arsenate minerals from the Arsenatnaya fumarole, Tolbachik volcano, Kamchatka, Russia. XXI. Magganasite, $CuFe^{3+}_3O(AsO_4)_3$

Igor V. Pekov[1]*, Natalia V. Zubkova[1], Atali A. Agakhanov[2], Natalia N. Koshlyakova[1], Nikita V. Chukanov[3], Vasiliy O. Yapaskurt[1], Sergey N. Britvin[4], Anna G. Turchkova[1], Elena S. Zhitova[5], Dmitry Yu. Pushcharovsky[1]

[1]Faculty of Geology, Moscow State University, Vorobievy Gory, 119991 Moscow, Russia

[2]Fersman Mineralogical Museum of the Russian Academy of Sciences, Leninsky Prospekt 18-2, 119071 Moscow, Russia

[3]Institute of Problems of Chemical Physics, Russian Academy of Sciences, Chernogolovka, Moscow region, 142432 Russia

[4]St. Petersburg State University, University Emb. 7/9, 199034 St. Petersburg, Russia

[5]Institute of Volcanology and Seismology, Far Eastern Branch of Russian Academy of Sciences, Piip Boulevard 9, 683006 Petropavlovsk-Kamchatsky, Russia

*E-mail: igorpekov@mail.ru

Running title: Magganasite, a new mineral

Abstract

The new mineral magganasite, ideally $CuFe^{3+}_3O(AsO_4)_3$, was found in the Arsenatnaya fumarole at the Second scoria cone of the Northern Breakthrough of the Great Tolbachik Fissure Eruption, Tolbachik volcano, Kamchatka, Russia. It is associated with sanidine, lammerite, paralammerite, johillerite, calciojohillerite, alarsite, hematite, tenorite, cassiterite, langbeinite, euchlorine, fedotovite, and wulffite. Magganasite forms prismatic crystals up to 0.2 mm long and up to 0.04 mm thick typically assembled in clusters up to 1 mm across. It is translucent, golden- or red-brown to brownish-yellow, with strong vitreous to semi-metallic lustre. D_{calc} is 4.708 g cm^{-3}. In reflected light, magganasite is grey, weakly anisotropic. The reflectance values [R_{max}–R_{min},% (λ, nm)] are: 13.1–13.1 (470), 12.5–11.9 (546), 12.2–11.9 (589), 11.9–11.8 (650). Chemical composition (wt.%, electron microprobe data) is: CuO 14.69, ZnO 0.06, Al_2O_3 0.49, Cr_2O_3 0.19, Fe_2O_3 30.62, TiO_2 2.22, SiO_2 0.21, P_2O_5 0.12, V_2O_5 0.10, As_2O_5 50.72, SO_3 0.63, total 100.05. The empirical formula based on 13 O *apfu* is $Cu_{1.22}Al_{0.06}Cr_{0.02}Fe^{3+}_{2.52}Ti_{0.18}(As_{2.91}S_{0.05}Si_{0.02}P_{0.01}V_{0.01})_{\sum 3.00}O_{13}$. Magganasite is triclinic, *P*-1, *a* = 5.1813(7), *b* = 9.6427(11), *c* = 9.6834(11) Å, α = 82.066(10), β = 78.680(11), γ = 79.962(10)°, *V* = 464.41(10) Å^3 and *Z* = 2. The strongest reflections of the PXRD pattern

[*d*,Å(*I*)(*hkl*)] are: 3.761(100)(102, 120), 3.540(46)(022), 3.280(88)(1-12), 3.204(62)(-120), 3.170(41)(-102, 030), 2.989(51)(-112), 2.889(65)(103, 130), and 2.510(64)(200). The crystal structure, solved from single-crystal XRD data (R = 0.0609), is unique. It is based on the polyhedral ribbons built by two zig-zag chains of edge-sharing Fe2- and Fe3-centred octahedra linked *via* dimers of edge-sharing Cu-centred distorted tetragonal pyramids. The neighboring ribbons are linked *via* dimers of edge-sharing Fe1-centred octahedra. AsO_4 tetrahedra reinforce the linkage between the ribbons. The mineral is named in honour of the Greek mineralogist and petrologist Prof. Dr. Andreas Magganas (born 1954).

Keywords: magganasite; new mineral; copper iron arsenate; crystal structure; fumarole sublimate; Tolbachik volcano.

Introduction

This article belongs to the series of papers devoted to new arsenate minerals from the Arsenatnaya fumarole at the Second scoria cone of the Northern Breakthrough of the Great Tolbachik Fissure Eruption 1975–1976 (NB GTFE), Tolbachik volcano, Kamchatka Peninsula, Far-Eastern Region, Russia. The descriptions of twenty three new mineral species were reported in the previous papers of the series: yurmarinite $Na_7(Fe^{3+},Mg,Cu)_4(AsO_4)_6$ (Pekov *et al.*, 2014a), two polymorphs of $Cu_4O(AsO_4)_2$, ericlaxmanite and kozyrevskite (Pekov *et al.*, 2014b), popovite $Cu_5O_2(AsO_4)_2$ (Pekov *et al.*, 2015a), structurally related shchurovskyite $K_2CaCu_6O_2(AsO_4)_4$ and dmisokolovite $K_3Cu_5AlO_2(AsO_4)_4$ (Pekov *et al.*, 2015b), katiarsite $KTiO(AsO_4)$ (Pekov *et al.*, 2016a), melanarsite $K_3Cu_7Fe^{3+}O_4(AsO_4)_4$ (Pekov *et al.*, 2016b), pharmazincite $KZnAsO_4$ (Pekov *et al.*, 2017), arsenowagnerite $Mg_2(AsO_4)F$ (Pekov *et al.*, 2018b), arsenatrotitanite $NaTiO(AsO_4)$ (Pekov *et al.*, 2019a), the two isostructural minerals edtollite $K_2NaCu_5Fe^{3+}O_2(AsO_4)_4$ and alumoedtollite $K_2NaCu_5AlO_2(AsO_4)_4$ (Pekov *et al.*, 2019b), anatolyite $Na_6(Ca,Na)(Mg,Fe^{3+})_3Al(AsO_4)_6$ (Pekov *et al.*, 2019c), zubkovaite $Ca_3Cu_3(AsO_4)_4$ (Pekov *et al.*, 2019d), pansnerite $K_3Na_3Fe^{3+}{}_6(AsO_4)_8$ (Pekov *et al.*, 2020a), badalovite $NaNaMg(MgFe^{3+})(AsO_4)_3$ (Pekov *et al.*, 2020b), calciojohillerite $NaCaMgMg_2(AsO_4)_3$ (Pekov *et al.*, 2021a), yurgensonite $K_2SnTiO_2(AsO_4)_2$ (Pekov *et al.*, 2021b), paraberzeliite $NaCaCaMg_2(AsO_4)_3$ (Pekov *et al.*, 2022a), khrenovite $Na_3Fe^{3+}{}_2(AsO_4)_3$ (Pekov *et al.*, 2022b), axelite $Na_{14}Cu_7(AsO_4)_8F_2Cl_2$ (Pekov *et al.*, 2023a), and evseevite $Na_2Mg(AsO_4)F$ (Pekov *et al.*, 2023b). All new Tolbachik minerals discovered prior 2020 are listed in (Pekov *et al.*, 2020c).

In this paper we describe the new mineral magganasite (Cyrillic: магганасит), ideally $CuFe^{3+}{}_3O(AsO_4)_3$. It is named in honour of the Greek mineralogist and petrologist Prof. Dr. Andreas Magganas (born 1954), Professor of Mineralogy, Petrology and Mineral Chemistry

https://doi.org/10.1180/mgm.2025.10141 Published online by Cambridge University Press

in National and Kapodistrian University of Athens, Greece, a specialist in volcanology and the mineralogy of volcanic fumaroles.

Both the new mineral and its name have been approved by the IMA Commission on New Minerals, Nomenclature and Classification (IMA CNMNC), IMA2021–112. The holotype specimen is deposited in the systematic collection of the Fersman Mineralogical Museum with the catalogue number 97913.

Occurrence and general appearance

The specimens with the new mineral described in this paper were collected by us in July 2021 in the Arsenatnaya fumarole located at the summit of the Second scoria cone of the NB GTFE. This scoria cone is a monogenetic volcano formed in 1975 (Fedotov and Markhinin, 1983) and Arsenatnaya is one of the largest and hottest Tolbachik fumaroles today, after almost a half of century after this formation. The temperatures in its deep levels measured by us using a chromel-alumel thermocouple in the period 2012–2022, reach 500°C. The mineralogy and zonation of sublimates of the Arsenatnaya fumarole were reported by Pekov *et al*. (2018a) and Shchipalkina *et al*. (2020); the brief mineralogical characterization of oxidizing-type fumaroles of Tolbachik was given by Vergasova and Filatov (2016) and Pekov *et al*. (2020c).

Magganasite was found in the material collected from hot (the temperature measured during sampling varied from 350 to 400°C) pockets situated 1–1.5 m below the day surface. It is closely associated with sanidine and lammerite. In some specimens, the new mineral is also associated with hematite, tenorite, paralammerite, johillerite, calciojohillerite, alarsite, langbeinite, euchlorine, fedotovite, wulffite, and cassiterite.

Magganasite forms prismatic crystals, elongated along [100], up to 0.07 mm (rarely up to 0.2 mm) long and up to 0.04 mm thick. Well-shaped crystals (Figure 1a) are rare; typically, the mineral occurs as crude crystals (Figures 1b-d). Slightly divergent crystals and skeletal, case-like individuals are common (Figures 1c-d). Magganasite crystals are typically assembled in near-parallel (Figure 1c) or chaotic (Figures 1b,d) clusters up to 1 mm across, separate or combined in crusts, usually interrupted, up to 1 mm × 3 mm. Magganasite overgrows lammerite and sanidine (Figure 2) which form encrustations on the surface of basalt scoria altered by fumarolic gas.

We believe that magganasite was deposited directly from the fumarolic gas as a volcanic sublimate at the temperatures not lower than 400ºC.

https://doi.org/10.1180/mgm.2025.10141 Published online by Cambridge University Press

Physical properties and optical data

Magganasite is translucent, with strong vitreous to semi-metallic lustre. It is golden-brown (visually resembling typical astrophyllite in colour) or yellow-brown to brownish-yellow in thin individuals and brown or reddish-brown in the largest massive clusters. The streak is yellow. Magganasite is brittle, cleavage or parting was not observed. The fracture is uneven. Density calculated using the empirical formula and unit-cell volume found from powder X-ray diffraction data is 4.708 g cm^{-3}.

Under the microscope in reflected light, magganasite is grey, pleochroism was not observed. Bireflectance is very weak, ΔR = 0.3% (589 nm). Anisotropy is weak, internal reflections were not observed. The reflectance values measured in air using the SiC standard (Zeiss, No. 545) are given in Table 1.

Infrared Spectroscopy

The infrared (IR) absorption spectrum of magganasite (Fig. 3) was obtained using an ALPHA FTIR spectrometer (Bruker Optics) with a resolution of 4 cm^{-1}. A total of 16 scans were obtained. Preliminarily, the sample was powdered, mixed with anhydrous KBr and pelletized. The IR spectrum of an analogous pellet of pure KBr was used as a reference.

The splitting of the bands of As–O stretching vibrations in the range 690 – 970 cm^{-1} reflects the presence of nonequivalent and strongly distorted AsO_4 tetrahedra in the crystal structure of magganasite. In such cases, As–O stretching vibrations cannot be divided into symmetric and asymmetric ones (Dultz *et al.*, 1975). The doublet 955+967 cm^{-1} corresponds to As–O stretching vibrations with a significant contribution of the As1–O2–Fe2 and As3–O12–Fe1 fragments with the shortest As–O bonds (1.634 and 1.630 Å, respectively) and relatively short Fe–O bonds (1.851 and 1.921 Å, respectively). The band at 907 cm^{-1} is tentatively assigned to stretching vibrations involving the As2–O5–Cu fragment with a somewhat longer As–O bond (1.669 Å) and the shortest Cu–O bond (1.920 Å).

In the range of 360 – 620 cm^{-1}, overlapping bands of Fe^{3+}–O- and Cu-O-stretching and O–As–O bending vibrations are observed. In particular, by analogy with the synthetic analogue of yaroshevskite $Cu_9O_2(VO_4)_4Cl_2$ (Siidra *et al.*, 2020), the bands at 619 and 549 cm^{-1} may correspond to stretching vibrations in which a major part of energy is concentrated on the shortest Cu–O5 and Cu–O3 bonds whereas other Cu–O and Fe–O bonds contribute to the absorption at ~460 cm^{-1}. However, admixed SO_4^{2-} anions and Ti–O bonds can absorb IR radiation with the wavenumber of 619 cm^{-1}.

https://doi.org/10.1180/mgm.2025.10141 Published online by Cambridge University Press

The weak bands at 1110, 1134, and 1195 cm^{-1} correspond to asymmetric stretching vibrations of SO_4 tetrahedra that are present in the mineral as a minor impurity (see below). The weak bands at 1655, 3338, and 3494 cm^{-1} are due to water impurity (adsorbed water and/or inclusions of a hydrous mineral).

The IR spectrum of magganasite is unique and can be used for the identification of this mineral. The absence of bands in the range from 1200 to 1600 cm^{-1} in the IR spectrum of magganasite indicates the absence of carbonate, orthoborate and nitrate groups.

Chemical composition

The chemical composition of magganasite was studied by EMPA using a Jeol JSM-6480LV scanning electron microscope equipped with an INCA-Wave 500 wavelength-dispersive spectrometer (Laboratory of Analytical Techniques of High Spatial Resolution, Dept. of Petrology, Moscow State University), with an acceleration voltage of 20 kV, a beam current of 20 nA, and a 3 μm beam diameter. The chemical data in wt.% and the used probe standards are reported in Table 2. Contents of other elements with atomic numbers >6 were below detection limits.

The empirical formula calculated on the basis of 13 O atoms per formula unit (*apfu*) is $(Cu_{1.22}Al_{0.06}Cr_{0.02}Fe^{3+}_{2.52}Ti_{0.18})_{\sum 4.00}(As_{2.91}S_{0.05}Si_{0.02}P_{0.01}V_{0.01})_{\sum 3.00}O_{13}$. The perfect stoichiometry of the empirical formula calculated by the anionic method confirms that all Fe is trivalent.

The simplified formula of magganasite is $Cu(Fe^{3+},Cu,Ti,Al)_3O[(As,S)O_4]_3$. The idealised formula is $CuFe^{3+}_3O(AsO_4)_3$ which requires CuO 11.98, Fe_2O_3 36.08, As_2O_5 51.94, total 100 wt.%.

X-ray crystallography and crystal structure determination details

Powder X-ray diffraction (XRD) data for magganasite (Table 3) were collected with a Rigaku R-AXIS Rapid II single-crystal diffractometer equipped with cylindrical image plate detector (radius 127.4 mm) using Debye-Scherrer geometry, Co*K*α radiation (rotating anode with VariMAX microfocus optics), 40 kV, 15 mA, and exposure 15 min. Angular resolution of the detector is 0.045º 2Θ (pixel size 0.1 mm). The data were integrated using the software package Osc2Tab (Britvin *et al*., 2017). The triclinic unit cell parameters calculated from the powder XRD data are: a = 5.18(1), b = 9.65(2), c = 9.69(2) Å, α = 82.06(5), β = 78.85(4), γ = 79.90(5)º, V = 464.7(6) $Å^3$.

https://doi.org/10.1180/mgm.2025.10141 Published online by Cambridge University Press

Single-crystal XRD studies of magganasite, including the obtaining of the dataset used for the structure determination, were carried out at room temperature using an Xcalibur S diffractometer equipped with a CCD detector (Mo*K*α-radiation). More than a hemisphere of three-dimensional data was collected. Data reduction was performed using CrysAlisPro Version 1.171.39.46 (Rigaku OD, 2018). The data were corrected for Lorentz factor and polarization effects. The crystal structure was solved by direct methods and refined using the SHELX software package (Sheldrick, 2015) to $R = 0.0609$ for 1987 reflections with $I > 2\sigma(I)$. The crystal data and the experimental details are presented in Table 4, atom coordinates and thermal displacement parameters in Tables 5 and 6, selected interatomic distances in Table 7 and bond valence calculations in Table 8.

Discussion

The crystal structure of magganasite (Fig. 4) is unique. It is based on the polyhedral ribbons elongated along the *a* axis and built by two zig-zag chains of edge-sharing Fe2- and Fe3-centred octahedra linked *via* dimers of edge-sharing Cu-centred distorted tetragonal pyramids. These dimers also share common edges with the octahedra belonging to the chains (Fig. 5a). The neighboring ribbons are linked *via* dimers of edge-sharing Fe1-centred octahedra (Fig. 5b). The Fe2 and Fe3 octahedra belonging to the ribbons and the Fe1-centred octahedra share common vertices to form the octahedral pseudo-framework. AsO_4 tetrahedra reinforce the linkage between the ribbons and share all oxygen vertices with *Me*-centred polyhedra (*Me* = Fe^{3+}, Cu^{2+}).

The structure of magganasite was studied on a crystal slightly enriched by Ti and Cu admixtures, that is $Cu_{1.38}$ and $Ti_{0.32}$ in *apfu*, in comparison with the average composition of the mineral reported in Table 2, $Cu_{1.22}$ and $Ti_{0.18}$ in *apfu*. The structure refinement was made ignoring minor (< 0.2 wt.% i.e. < 0.03 *apfu*) admixtures Zn, Cr, Si, P, and V and the following crystal chemical formula was obtained from the structure data: $^{Cu}Cu^{Fe1}(Fe_{0.68}Ti_{0.32})^{Fe2}(Fe_{0.62}Cu_{0.38})^{Fe3}(Fe_{0.99}Al_{0.01})O[^{As1–3}(As_{2.94}S_{0.06})O_{12}]$ (Tables 4 and 5).

Trivalent state of iron in magganasite (Table 2) is clearly confirmed by interatomic distances Fe1,2,3–O (Table 7), bond valence sums (BVS) for all Fe sites (Table 8) and the empirical formula calculation (see above). This is in a good agreement with strongly oxidizing conditions of the mineral formation in the Arsenatnaya fumarole (Pekov *et al.*, 2018a, 2020c). Calculation of the distortion index in the octahedra was performed using a VESTA 3 program (Momma and Izumi, 2011) and showed that Fe3-centred octahedron has the lowest value of the distortion index (0.035) whereas Fe2- and Fe1-centred octahedra are

https://doi.org/10.1180/mgm.2025.10141 Published online by Cambridge University Press

characterized by higher values: 0.050 and 0.054, respectively. This, together with refined number of electrons (e_{ref} = 27.66 with Fe scattering curve used for the refinement) and the lowest BVS value (2.52 v.u.) for the Fe2 site (Table 8), undoubtedly confirmed that all Cu^{2+} excess over 1 *apfu* occurs at Fe2 (Table 5). The highest BVS value (3.31 v.u.) for the Fe1 site (Table 8), the lowest refined number of electrons (e_{ref} = 24.39), and a high value of the distortion index demonstrated that admixed Ti^{4+} occurs in Fe1. For the Fe3 site, BVS = 2.98 v.u. (Table 5) and e_{ref} = 25.92; taking into account that admixed Cu and Ti occur in the Fe2 and Fe1 sites, respectively, we concluded that Fe3 is populated almost exclusively by Fe^{3+}.

Thus, magganasite is unique in terms of crystal chemistry; no data on a structurally related mineral or synthetic compound are found in literature and databases. The only known H-free natural arsenate with only Cu and Fe as species-defining metal cations, auriacusite $CuFe^{3+}O(AsO_4)$, a member of the olivenite group (Mills *et al.*, 2010) differs from magganasite in stoichiometry, symmetry, unit-cell data and crystal structure, as well as in genesis: auriacusite occurs in the oxidation zone of sulfide ores. Beershevaite $CaFe^{3+}{}_3O(PO_4)_3$, a recently discovered mineral from paralavas of the Hatrurim formation, Israel (IMA2020–095a: Britvin *et al.*, 2021) is a Ca-Fe^{3+} phosphate with the same type of formula as magganasite $CuFe^{3+}{}_3O(AsO_4)_3$, however, these minerals are different in symmetry, unit-cell metrics and crystal structure.

Acknowledgements

We thank M. Akasaka and two anonymous referees for their valuable comments. The mineralogical and crystal chemical studies of magganasite were supported by the Russian Science Foundation, grant no. 25-17-00005. The IR spectroscopic investigation was performed in accordance with the state task, registration number 124013100858-3. The powder XRD study was performed at the Center for X-Ray Diffraction Research of the Science Park of St. Petersburg State University within the framework of project 125021702335-5.

References

Britvin S.N., Dolivo-Dobrovolsky D.V. and Krzhizhanovskaya M.G. (2017) Software for processing the X-ray powder diffraction data obtained from the curved image plate detector of Rigaku RAXIS Rapid II diffractometer. *Zapiski Rossiiskogo Mineralogicheskogo Obshchestva*, **146**, 104–107 (in Russian).

Clark R.C. and Reid J.S. (1995) The analytical calculation of absorption correction in multifaceted crystals. *Acta Crystallographica*, **A51**, 887–897.

https://doi.org/10.1180/mgm.2025.10141 Published online by Cambridge University Press

Dultz W., Quilichini M., Scott J.F. and Lehmann G. (1975) Phonon spectra of quartz isomorphs. *Physical Reviews B*, **11**, 1648–1653.

Fedotov S.A. and Markhinin Y.K., eds. (1983) *The Great Tolbachik Fissure Eruption*. Cambridge University Press, New York, 341 pp.

Gagné O.C. and Hawthorne F.C. (2015) Comprehensive derivation of bond-valence parameters for ion pairs involving oxygen. *Acta Crystallographica*, B**71**, 562–578.

Mills S.J., Kampf A.R., Poirier G., Raudsepp M. and Steele I.M. (2010) Auriacusite, $Fe^{3+}Cu^{2+}AsO_4O$, the first M^{3+} member of the olivenite group, from the Black Pine mine, Montana, USA. *Mineralogy and Petrology*, **99**, 113–120.

Momma K. and Izumi F. (2011) VESTA 3 for three-dimensional visualization of crystal, volumetric and morphology data. *Journal of Applied Crystallography*, **44**, 1272-1276.

Pekov I.V., Zubkova N.V., Yapaskurt V.O., Belakovskiy D.I., Lykova I.S., Vigasina M.F., Sidorov E.G. and Pushcharovsky D.Yu. (2014a) New arsenate minerals from the Arsenatnaya fumarole, Tolbachik volcano, Kamchatka, Russia. I. Yurmarinite, $Na_7(Fe^{3+},Mg,Cu)_4(AsO_4)_6$. *Mineralogical Magazine*, **78**, 905–917.

Pekov I.V., Zubkova N.V., Yapaskurt V.O., Belakovskiy D.I., Vigasina M.F., Sidorov E.G. and Pushcharovsky D.Yu. (2014b) New arsenate minerals from the Arsenatnaya fumarole, Tolbachik volcano, Kamchatka, Russia. II. Ericlaxmanite and kozyrevskite, two natural modifications of $Cu_4O(AsO_4)_2$. *Mineralogical Magazine*, **78**, 1527–1543.

Pekov I.V., Zubkova N.V., Yapaskurt V.O., Belakovskiy D.I., Vigasina M.F., Sidorov E.G. and Pushcharovsky D.Yu. (2015a) New arsenate minerals from the Arsenatnaya fumarole, Tolbachik volcano, Kamchatka, Russia. III. Popovite, $Cu_5O_2(AsO_4)_2$. *Mineralogical Magazine*, **79**, 133–143.

Pekov I.V., Zubkova N.V., Belakovskiy D.I., Yapaskurt V.O., Vigasina M.F., Sidorov E.G. and Pushcharovsky D.Yu. (2015b) New arsenate minerals from the Arsenatnaya fumarole, Tolbachik volcano, Kamchatka, Russia. IV. Shchurovskyite, $K_2CaCu_6O_2(AsO_4)_4$, and dmisokolovite, $K_3Cu_5AlO_2(AsO_4)_4$. *Mineralogical Magazine*, **79**, 1737–1753.

Pekov I.V., Yapaskurt V.O., Britvin S.N., Zubkova N.V., Vigasina M.F. and Sidorov E.G. (2016a) New arsenate minerals from the Arsenatnaya fumarole, Tolbachik volcano, Kamchatka, Russia. V. Katiarsite, $KTiO(AsO_4)$. *Mineralogical Magazine*, **80**, 639–646.

Pekov I.V., Zubkova N.V., Yapaskurt V.O., Polekhovsky Yu.S., Vigasina M.F., Belakovskiy D.I., Britvin S.N., Sidorov E.G. and Pushcharovsky D.Yu. (2016b) New arsenate minerals from the Arsenatnaya fumarole, Tolbachik volcano, Kamchatka, Russia. VI. Melanarsite, $K_3Cu_7Fe^{3+}O_4(AsO_4)_4$. *Mineralogical Magazine*, **80**, 855–867.

https://doi.org/10.1180/mgm.2025.10141 Published online by Cambridge University Press

Pekov I.V., Yapaskurt V.O., Belakovskiy D.I., Vigasina M.F., Zubkova N.V. and Sidorov E.G. (2017) New arsenate minerals from the Arsenatnaya fumarole, Tolbachik volcano, Kamchatka, Russia. VII. Pharmazincite, $KZnAsO_4$. *Mineralogical Magazine*, **81**, 1001–1008.

Pekov I.V., Koshlyakova N.N., Zubkova N.V., Lykova I.S., Britvin S.N., Yapaskurt V.O., Agakhanov A.A., Shchipalkina N.V., Turchkova A.G. and Sidorov E.G. (2018a) Fumarolic arsenates – a special type of arsenic mineralization. *European Journal of Mineralogy*, **30**, 305–322.

Pekov I.V., Zubkova N.V., Agakhanov A.A., Yapaskurt V.O., Chukanov N.V., Belakovskiy D.I., Sidorov E.G. and Pushcharovsky D.Yu. (2018b) New arsenate minerals from the Arsenatnaya fumarole, Tolbachik volcano, Kamchatka, Russia. VIII. Arsenowagnerite, $Mg_2(AsO_4)F$. *Mineralogical Magazine*, **82**, 877–888.

Pekov I.V., Zubkova N.V., Agakhanov A.A., Belakovskiy D.I., Vigasina M.F., Yapaskurt V.O., Sidorov E.G., Britvin S.N. and Pushcharovsky D.Y. (2019a) New arsenate minerals from the Arsenatnaya fumarole, Tolbachik volcano, Kamchatka, Russia. IX. Arsenatrotitanite, $NaTiO(AsO_4)$. *Mineralogical Magazine*, **83**, 453–458.

Pekov I.V., Zubkova N.V., Agakhanov A.A., Ksenofontov D.A., Pautov L.A., Sidorov E.G., Britvin S.N., Vigasina M.F. and Pushcharovsky D.Yu. (2019b) New arsenate minerals from the Arsenatnaya fumarole, Tolbachik volcano, Kamchatka, Russia. X. Edtollite, $K_2NaCu_5Fe^{3+}O_2(AsO_4)_4$, and alumoedtollite, $K_2NaCu_5AlO_2(AsO_4)_4$. *Mineralogical Magazine*, **83**, 485–495.

Pekov I.V., Lykova I.S., Yapaskurt V.O., Belakovskiy D.I., Turchkova A.G., Britvin S.N., Sidorov E.G. and Scheidl K.S. (2019c) New arsenate minerals from the Arsenatnaya fumarole, Tolbachik volcano, Kamchatka, Russia. XI. Anatolyite, $Na_6(Ca,Na)(Mg,Fe^{3+})_3Al(AsO_4)_6$. *Mineralogical Magazine*, **83**, 633–638.

Pekov I.V., Lykova I.S., Agakhanov A.A., Belakovskiy D.I., Vigasina M.F., Britvin S.N., Turchkova A.G., Sidorov E.G. and Scheidl K.S. (2019d) New arsenate minerals from the Arsenatnaya fumarole, Tolbachik volcano, Kamchatka, Russia. XII. Zubkovaite, $Ca_3Cu_3(AsO_4)_4$. *Mineralogical Magazine*, **83**, 879–886.

Pekov I.V., Zubkova N.V., Koshlyakova N.N., Agakhanov A.A., Belakovskiy D.I., Vigasina M.F., Yapaskurt V.O., Britvin S.N., Turchkova A.G., Sidorov E.G. and Pushcharovsky D.Y. (2020a) New arsenate minerals from the Arsenatnaya fumarole, Tolbachik volcano, Kamchatka, Russia. XIII. Pansnerite, $K_3Na_3Fe^{3+}{}_6(AsO_4)_8$. *Mineralogical Magazine*, **84**, 143–151.

https://doi.org/10.1180/mgm.2025.10141 Published online by Cambridge University Press

Pekov I.V., Koshlyakova N.N., Agakhanov A.A., Zubkova N.V., Belakovskiy D.I., Vigasina M.F., Turchkova A.G., Sidorov E.G. and Pushcharovsky D.Yu. (2020b) New arsenate minerals from the Arsenatnaya fumarole, Tolbachik volcano, Kamchatka, Russia. XIV. Badalovite, $NaNaMg(MgFe^{3+})(AsO_4)_3$, a member of the alluaudite group. *Mineralogical Magazine*, **84**, 616–622.

Pekov I.V., Agakhanov A.A., Zubkova N.V., Koshlyakova N.V., Shchipalkina N.V., Sandalov F.D., Yapaskurt V.O., Turchkova A.G. and Sidorov E.G. (2020c) Oxidizing-type fumaroles of the Tolbachik Volcano, a mineralogical and geochemical unique. *Russian Geology and Geophysics*, **61**, 675–688.

Pekov I.V., Koshlyakova N.N., Agakhanov A.A., Zubkova N.V., Belakovskiy D.I., Vigasina M.F., Turchkova A.G., Sidorov E.G. and Pushcharovsky D.Yu. (2021a) New arsenate minerals from the Arsenatnaya fumarole, Tolbachik volcano, Kamchatka, Russia. XV. Calciojohillerite, $NaCaMgMg_2(AsO_4)_3$, a member of the alluaudite group. *Mineralogical Magazine*, **85**, 215–223.

Pekov I.V., Zubkova N.V., Agakhanov A.A., Yapaskurt V.O., Belakovskiy D.I., Vigasina M.F., Britvin S.N., Turchkova A.G., Sidorov E.G. and Pushcharovsky D.Yu. (2021b) New arsenate minerals from the Arsenatnaya fumarole, Tolbachik volcano, Kamchatka, Russia. XVI. Yurgensonite, $K_2SnTiO_2(AsO_4)_2$, the first natural tin arsenate, and the katiarsite–yurgensonite isomorphous series. *Mineralogical Magazine*, **85**, 698–707.

Pekov I.V., Koshlyakova N.N., Belakovskiy D.I., Vigasina M.F., Zubkova N.V., Agakhanov A.A., Britvin S.N., Sidorov E.G. and Pushcharovsky D.Yu. (2022a) New arsenate minerals from the Arsenatnaya fumarole, Tolbachik volcano, Kamchatka, Russia. XVII. Paraberzeliite, $NaCaCaMg_2(AsO_4)_3$, an alluaudite-group member dimorphous with berzeliite. *Mineralogical Magazine*, **86**, 103–111.

Pekov I.V., Koshlyakova N.N., Belakovskiy D.I., Vigasina M.F., Zubkova N.V., Agakhanov A.A., Britvin S.N., Sidorov E.G. and Pushcharovsky D.Yu. (2022b) New arsenate minerals from the Arsenatnaya fumarole, Tolbachik volcano, Kamchatka, Russia. XVIII. Khrenovite, $Na_3Fe^{3+}{}_2(AsO_4)_3$, the sodium-richest alluaudite-group member. *Mineralogical Magazine*, **86**, 897–902.

Pekov I.V., Zubkova N.V., Agakhanov A.A., Yapaskurt V.O., Belakovskiy D.I., Britvin S.N., Sidorov E.G., Kutyrev A.V. and Pushcharovsky D.Yu. (2023a) New arsenate minerals from the Arsenatnaya fumarole, Tolbachik volcano, Kamchatka, Russia. XIX. Axelite, $Na_{14}Cu_7(AsO_4)_8F_2Cl_2$. *Mineralogical Magazine*, **87**, 109–117.

https://doi.org/10.1180/mgm.2025.10141 Published online by Cambridge University Press

Pekov I.V., Zubkova N.V., Agakhanov A.A., Vigasina M.F., Yapaskurt V.O., Britvin S.N., Turchkova A.G., Sidorov E.G., Zhitova E.S. and Pushcharovsky D.Yu. (2023b) New arsenate minerals from the Arsenatnaya fumarole, Tolbachik volcano, Kamchatka, Russia. XX. Evseevite, $Na_2Mg(AsO_4)F$, the first natural arsenate with antiperovskite structure . *Mineralogical Magazine*, **87**, 839–848.

Rigaku Oxford Diffraction (2018) *CrysAlisPro Software System, v. 1.171.39.46*, Rigaku Corporation, Oxford, UK.

Shchipalkina N.V., Pekov I.V., Koshlyakova N.N., Britvin S.N., Zubkova N.V., Varlamov D.A. and Sidorov E.G. (2020) Unusual silicate mineralization in fumarolic sublimates of the Tolbachik volcano, Kamchatka, Russia – Part 1: Neso-, cyclo-, ino- and phyllosilicates. *European Journal of Mineralogy*, **32**, 101–119.

Sheldrick G.M. (2015) Crystal structure refinement with SHELXL. *Acta Crystallographica*, **C71**, 3–8.

Siidra O.I., Vladimirova V.A., Tsirlin A.A., Chukanov N.V. and Ugolkov V.L. (2020) $Cu_9O_2(VO_4)_4Cl_2$, the first copper oxychloride vanadate: Mineralogically inspired synthesis and large spin canting. *Inorganic Chemistry*, **59**, 2136–2143.

Vergasova L.P. and Filatov S.K. (2016) A study of volcanogenic exhalation mineralization. *Journal of Volcanology and Seismology*, **10(2)**, 71–85.

https://doi.org/10.1180/mgm.2025.10141 Published online by Cambridge University Press

Table 1. The reflectance data of magganasite,

λ (nm)	R_{max}, %	R_{min}, %	λ (nm)	R_{max}, %	R_{min}, %
400	15.4	14.7	560	12.4	11.9
420	14.6	13.7	580	12.3	11.1
440	13.8	13.2	**589**	**12.2**	**11.9**
460	13.3	13.2	600	12.2	11.9
470	**13.1**	**13.1**	620	12.1	11.9
480	13.1	12.8	640	11.9	11.9
500	12.9	12.3	**650**	**11.9**	**11.8**
520	12.7	12.1	660	11.8	11.7
540	12.5	11.9	680	11.8	11.5
546	**12.5**	**11.9**	700	11.6	11.3

The values for wavelengths (λ) recommended by the IMA Commission on Ore Mineralogy are marked in boldtype.

Table 2. Chemical composition of magganasite.

Constituent	Average, wt.%*	Range, wt.%	SD, wt.%	Probe standard	*apfu***
CuO	14.69	12.81 – 17.65	1.15	$CuFeS_2$	Cu 1.22
ZnO	0.06	0.00 – 0.30	0.06	ZnS	Zn 0.00
Al_2O_3	0.49	0.19 – 0.82	0.19	Al_2O_3	Al 0.06
Cr_2O_3	0.19	0.00 – 0.41	0.09	Cr	Cr 0.02
Fe_2O_3	30.62	25.04 – 33.60	2.02	$CuFeS_2$	Fe^{3+} 2.52
TiO_2	2.22	0.87 – 5.31	1.12	ilmenite	Ti 0.18
SiO_2	0.21	0.05 – 0.72	0.21	diopside	Si 0.02
P_2O_5	0.12	0.00 – 0.24	0.07	$KTiOPO_4$	P 0.01
V_2O_5	0.10	0.01 – 0.31	0.08	V	V 0.01
As_2O_5	50.72	49.97 – 51.85	0.48	GaAs	As 2.91
SO_3	0.63	0.00 – 1.24	0.37	FeS_2	S 0.05
Total	100.05				

*Averaged for 15 spot analyses. **Atoms per formula unit calculated on the basis of 13 O atoms per formula unit. SD – standard deviation.

https://doi.org/10.1180/mgm.2025.10141 Published online by Cambridge University Press

Table 3. Powder X-ray diffraction data (d in Å) of magganasite.

I_{obs}	d_{obs}	I_{calc}*	d_{calc}**	$h\ k\ l$		I_{obs}	d_{obs}	I_{calc}*	d_{calc}**	$h\ k\ l$
6	9.47	4	9.440	010		15	2.132	7	2.148	1-14
6	5.01	3	5.022	100				2	2.133	223
11	4.749	11	4.720	020				2	2.126	230
15	4.694	6	4.671	111				5	2.123	232
3	4.423	2	4.416	021		11	2.120	8	2.114	0-33
15	4.170	9	4.179	-110		9	2.030	2	2.031	134
6	4.047	4	4.051	0-21				4	2.027	143
6	3.920	3	3.905	-1-11				7	2.026	0-42
100	**3.761**	20	3.789	102		6	2.000	2	2.004	-104
		8	3.761	121				3	1.994	043
		57	3.733	120		6	1.975	1	1.977	233
46	**3.540**	40	3.533	022				3	1.973	-114
88	**3.280**	100	3.295	1-12		12	1.961	3	1.956	-133
62	**3.204**	46	3.205	-120				8	1.953	-2-22
41	**3.170**	9	3.171	-102		15	1.881	9	1.895	204
		19	3.147	030				4	1.891	051
25	3.081	22	3.086	031				3	1.880	242
36	3.037	27	3.028	-1-12		3	1.846	4	1.844	1-42
51	**2.989**	37	2.985	-112		5	1.831	4	1.832	-230
26	2.925	9	2.938	113				4	1.826	2-23
		11	2.911	131		9	1.815	2	1.822	052
65	**2.889**	18	2.907	103				1	1.813	-203
		3	2.893	0-31				5	1.811	144
		40	2.869	130		11	1.797	11	1.798	0-43
28	2.762	29	2.759	032		5	1.787	4	1.790	2-14
31	2.690	31	2.702	1-22		4	1.770	3	1.765	-213
27	2.678	24	2.661	-1-22		2	1.743	1	1.745	135
15	2.612	1	2.605	-1-31				1	1.739	153
		12	2.604	-122		5	1.723	1	1.727	311
2	2.569	1	2.574	211				2	1.720	-2-23
64	**2.510**	58	2.511	200				3	1.717	-143
14	2.485	6	2.497	0-32		8	1.697	1	1.700	-1-43
		7	2.477	-103				2	1.697	321
7	2.436	5	2.445	212				7	1.691	0-52
		1	2.430	221		9	1.676	2	1.685	1-43
9	2.393	2	2.399	202				4	1.681	322
		5	2.390	-1-13				1	1.674	300

https://doi.org/10.1180/mgm.2025.10141 Published online by Cambridge University Press

34	2.357	32	2.360	040		8	1.663	3	1.668	251
		7	2.355	033				3	1.666	-223
10	2.331	6	2.335	222				3	1.659	320
		11	2.328	114		3	1.646	3	1.648	2-24
19	2.210	7	2.212	1-32		16	1.605	2	1.606	-152
		3	2.208	042				5	1.603	116
		3	2.208	-132				10	1.603	-240
								10	1.602	154

Table 3. Continued.

I_{obs}	d_{obs}	I_{calc}*	d_{calc}**	*h k l*		I_{obs}	d_{obs}	I_{calc}*	d_{calc}**	*h k l*
19	1.589	11	1.597	3-12		12	1.472	9	1.472	063
		2	1.586	0-44				7	1.470	-3-22
		5	1.586	-204		11	1.463	4	1.463	1-53
		4	1.583	106				2	1.462	261
10	1.554	5	1.558	-214		9	1.456	6	1.456	262
		6	1.551	-144				5	1.455	-312
6	1.542	9	1.543	062				4	1.452	-2-52
		2	1.539	-233		11	1.424	5	1.426	-116
14	1.519	6	1.526	314				13	1.425	236
		9	1.526	0-61				4	1.423	-1-62
		2	1.523	1-16		9	1.403	1	1.406	315
		2	1.518	324				1	1.406	-243
5	1.502	1	1.505	-1-44				8	1.404	-1-16
		2	1.497	-302						
		4	1.496	2-34						

*For the calculated pattern (calculated using the WinXPOW v. 2.2 software) only reflections with intensities ≥1 are given; **for the unit-cell parameters calculated from single-crystal data. The strongest reflections are marked in boldtype.

https://doi.org/10.1180/mgm.2025.10141 Published online by Cambridge University Press

Table 4. Crystal data, data collection information and structure refinement details for magganasite.

Formula (according to structural data)	$Cu^{2+}(Fe^{3+}_{0.68}Ti_{0.32})(Fe^{3+}_{0.62}Cu^{2+}_{0.38})(Fe^{3+}_{0.99}Al_{0.01})O[(As_{2.94}S_{0.06})O_{12}]$
Formula weight	661.15
Temperature, K	293(2)
Radiation and wavelength, Å	Mo*K*α; 0.71073
Crystal system, space group, *Z*	Triclinic, *P*-1, 2
Unit cell dimensions, Å/°	*a* = 5.1813(7) α = 82.066(10) *b* = 9.6427(11) β = 78.680(11) *c* = 9.6834(11) γ = 79.962(10)
V, Å^3	464.41(10)
Absorption coefficient μ, mm^{-1}	17.364
F_{000}	617
Crystal size, mm^3	0.02 × 0.03 × 0.11
Diffractometer	Xcalibur S CCD
θ range for data collection, ° / Collection mode	4.30 – 28.05 / hemisphere
Reflections collected	3750
Index ranges	$-5 \le h \le 6$, $-12 \le k \le 7$, $-12 \le l \le 12$
Reflections with $I > 2\sigma(I)$	1987
Data reduction	CrysAlisPro Version 1.171.39.46 (Rigaku OD, 2018)
Absorption correction	Analytical (Clark and Reid, 1995)
Structure solution	direct methods
Refinement method	full-matrix least-squares on F^2
Number of refined parameters	167
Final *R* indices [$I>2\sigma(I)$]	*R*1 = 0.0609, w*R*2* = 0.0953
R indices (all data)	*R*1 = 0.1325, w*R*2* = 0.1091
GoF	0.890
Largest diff. peak and hole, e/Å^3	1.758 and -1.824

* $w = 1/[\sigma^2(F_o^2) + (0.0383P)^2]$; $P = ([\text{max of } (0 \text{ or } F_o^2)] + 2F_c^2)/3$

https://doi.org/10.1180/mgm.2025.10141 Published online by Cambridge University Press

Table 5. Coordinates and equivalent displacement parameters (U_{eq}, in Å^2) of atoms in magganasite.

Site	*x*	*y*	*z*	U_{eq}	Site occupancy
As1	0.3070(3)	0.92637(17)	0.23172(15)	0.0063(5)	$As_{0.954(12)}S_{0.046(12)}$**
As2	0.7638(3)	0.67238(16)	0.50014(16)	0.0077(5)	$As_{1.00}$
As3	0.2382(3)	0.34581(17)	-0.00147(16)	0.0054(5)	$As_{0.982(12)}S_{0.018(12)}$**
Cu	0.2137(3)	0.8946(2)	0.5663(2)	0.0166(6)	$Cu_{1.00}$
Fe1	0.2109(4)	0.8801(2)	0.9079(2)	0.0071(8)	$Fe_{0.68(4)}Ti_{0.32(4)}$***
Fe2	0.2218(3)	0.5970(2)	0.2129(2)	0.0091(7)	$Fe_{0.62(5)}Cu_{0.38(5)}$
Fe3	0.2221(4)	0.5947(2)	0.7141(2)	0.0099(7)	$Fe_{0.992(15)}Al_{0.008(15)}$
O1	0.2245(17)	0.7838(11)	0.7522(9)	0.013(2)	$O_{1.00}$
O2	0.3177(18)	0.7550(11)	0.2669(10)	0.014(2)	$O_{1.00}$
O3	0.1346(17)	0.9955(11)	0.3764(10)	0.013(2)	$O_{1.00}$
O4	0.1391(16)	0.9871(10)	0.0972(9)	0.009(2)	$O_{1.00}$
O5	0.5759(16)	0.8309(10)	0.4834(10)	0.010(2)	$O_{1.00}$
O6	0.8630(16)	0.5968(10)	0.3465(10)	0.008(2)	$O_{1.00}$
O7	0.3854(16)	0.4634(10)	-0.1221(10)	0.007(2)	$O_{1.00}$
O8	0.5974(17)	0.5578(11)	0.6198(10)	0.014(2)	$O_{1.00}$
O9	0.0424(17)	0.6895(11)	0.5562(10)	0.013(2)	$O_{1.00}$
O10	-0.0211(16)	0.2854(10)	-0.0450(9)	0.007(2)*	$O_{1.00}$
O11	0.6110(16)	0.9677(10)	0.1982(9)	0.009(2)*	$O_{1.00}$
O12	0.4632(17)	0.2110(10)	0.0318(10)	0.011(2)*	$O_{1.00}$
O13	0.1203(16)	0.4277(10)	0.1477(10)	0.007(2)*	$O_{1.00}$

*U_{iso}; **"S" in fact means S + minor Si, P and V; ***"Ti" in fact means Ti + minor Al and Cr.

Table 6. Anisotropic displacement parameters of atoms in the structure of magganasite.

Site	U_{11}	U_{22}	U_{33}	U_{23}	U_{13}	U_{12}
As1	0.0034(8)	0.0091(9)	0.0064(9)	-0.0019(6)	-0.0011(6)	-0.0002(6)
As2	0.0050(8)	0.0092(9)	0.0093(9)	-0.0034(7)	-0.0011(6)	-0.0011(6)
As3	0.0028(8)	0.0063(9)	0.0077(9)	-0.0018(6)	-0.0010(6)	-0.0012(6)
Cu	0.0102(11)	0.0229(13)	0.0122(11)	-0.0001(9)	-0.0001(7)	0.0063(8)
Fe1	0.0039(12)	0.0099(15)	0.0075(14)	0.0000(10)	-0.0018(9)	-0.0010(9)
Fe2	0.0063(12)	0.0086(12)	0.0129(13)	-0.0049(9)	-0.0007(8)	-0.0006(8)
Fe3	0.0066(12)	0.0143(14)	0.0081(13)	-0.0002(9)	-0.0002(8)	-0.0016(9)
O1	0.015(6)	0.024(7)	0.003(5)	-0.002(5)	-0.001(4)	-0.014(5)
O2	0.023(6)	0.009(6)	0.014(6)	-0.007(5)	-0.009(4)	-0.001(4)
O3	0.005(5)	0.020(6)	0.014(6)	-0.003(5)	0.000(4)	0.001(4)
O4	0.006(5)	0.005(6)	0.015(6)	-0.002(4)	0.003(4)	0.000(4)
O5	0.004(5)	0.014(6)	0.011(6)	-0.004(4)	-0.003(4)	0.003(4)
O6	0.004(5)	0.002(5)	0.018(6)	0.001(4)	-0.005(4)	-0.001(4)
O7	0.005(5)	0.004(5)	0.011(6)	-0.002(4)	0.001(4)	0.000(4)
O8	0.007(5)	0.012(6)	0.020(6)	-0.009(5)	0.009(4)	-0.004(4)
O9	0.010(5)	0.019(6)	0.011(6)	0.000(5)	-0.005(4)	-0.003(4)

https://doi.org/10.1180/mgm.2025.10141 Published online by Cambridge University Press

Table 7. Selected interatomic distances (Å) in the structure of magganasite.

As1 - O2 1.634(10)	Fe1 - O1 1.861(9)
- O11 1.652(8)	- O12 1.921(9)
- O3 1.662(9)	- O11 1.935(9)
- O4 1.689(9)	- O4 2.035(9)
<As1 - O> 1.659	- O4 2.163(9)
As2 - O5 1.669(9)	- O10 2.174(9)
- O9 1.680(8)	<Fe1 - O> 2.015
- O6 1.697(9)	Fe2 - O2 1.851(10)
- O8 1.701(9)	- O13 2.014(9)
<As1 - O> 1.687	- O6 2.046(9)
As3 - O12 1.630(9)	- O7 2.069(8)
- O7 1.678(9)	- O10 2.181(9)
- O10 1.698(8)	- O8 2.274(10)
- O13 1.698(9)	<Fe2 - O> 2.073
<As1 - O> 1.676	Fe3 - O1 1.913(10)
Cu - O5 1.920(9)	- O8 1.973(9)
- O3 1.947(9)	- O9 1.979(9)
- O1 1.967(10)	- O13 2.027(9)
- O3 2.040(10)	- O7 2.106(9)
- O9 2.326(10)	- O6 2.152(9)
<Cu - O> 2.04	<Fe3 - O> 2.025

Table 8. Bond valence calculations for magganasite. Bond-valence parameters were taken from Gagné and Hawthorne (2015).

	As1	As2	As3	Cu	Fe1	Fe2	Fe3	Σ
O1				0.45	0.80		0.66	1.91
O2	1.43					0.73		2.16
O3	1.32			0.48 0.37				2.17
O4	1.22				0.49 0.35			2.06
O5		1.31		0.52				1.83
O6		1.21				0.42	0.34	1.97
O7			1.28			0.40	0.39	2.07
O8		1.20				0.22	0.56	1.98
O9		1.27		0.17			0.55	1.99
O10			1.21		0.33	0.29		1.83
O11	1.36				0.66			2.02
O12			1.46		0.68			2.14
O13			1.21			0.46	0.48	2.15
Σ	5.33	4.99	5.16	1.99	3.31	2.52	2.98	

https://doi.org/10.1180/mgm.2025.10141 Published online by Cambridge University Press

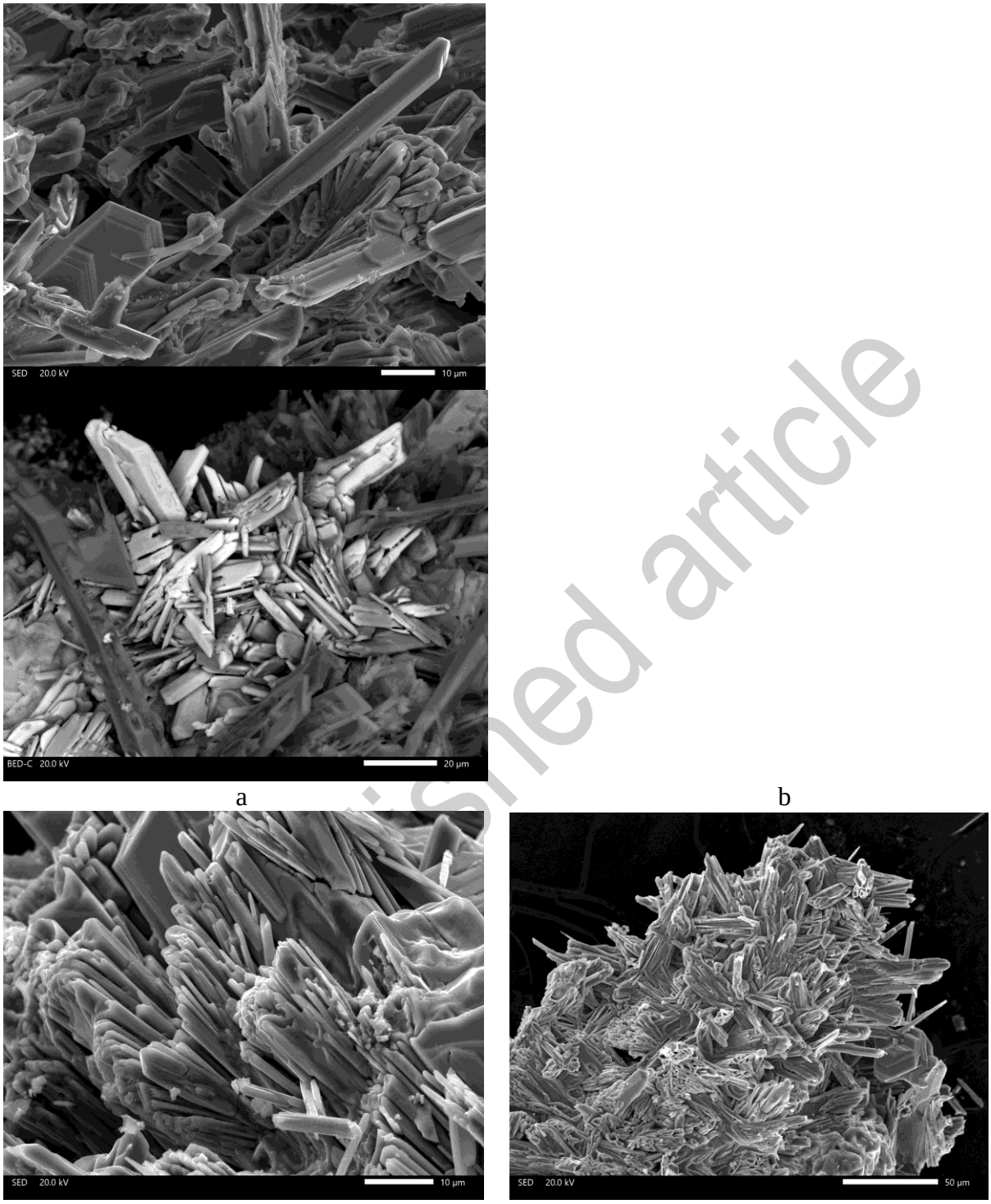

Figure 1. Morphology of magganasite crystals and aggregates: a (holotype) – well-shaped long-prismatic crystal of magganasite on aggregate of its crude prismatic crystals (hexagonal tabular crystal in left part of the image is lammerite); b – group of prismatic magganasite crystals (white) on crystal crust of sanidine (grey) and lammerite (light grey, in left part of the image); c – near-parallel intergrowths of slightly divergent prismatic magganasite crystals; d

https://doi.org/10.1180/mgm.2025.10141 Published online by Cambridge University Press

– chaotic aggregate of prismatic magganasite crystals (hexagonal tabular crystal in right part of the image is lammerite). SEM images, SE (a, c, d) and BSE (b) modes.

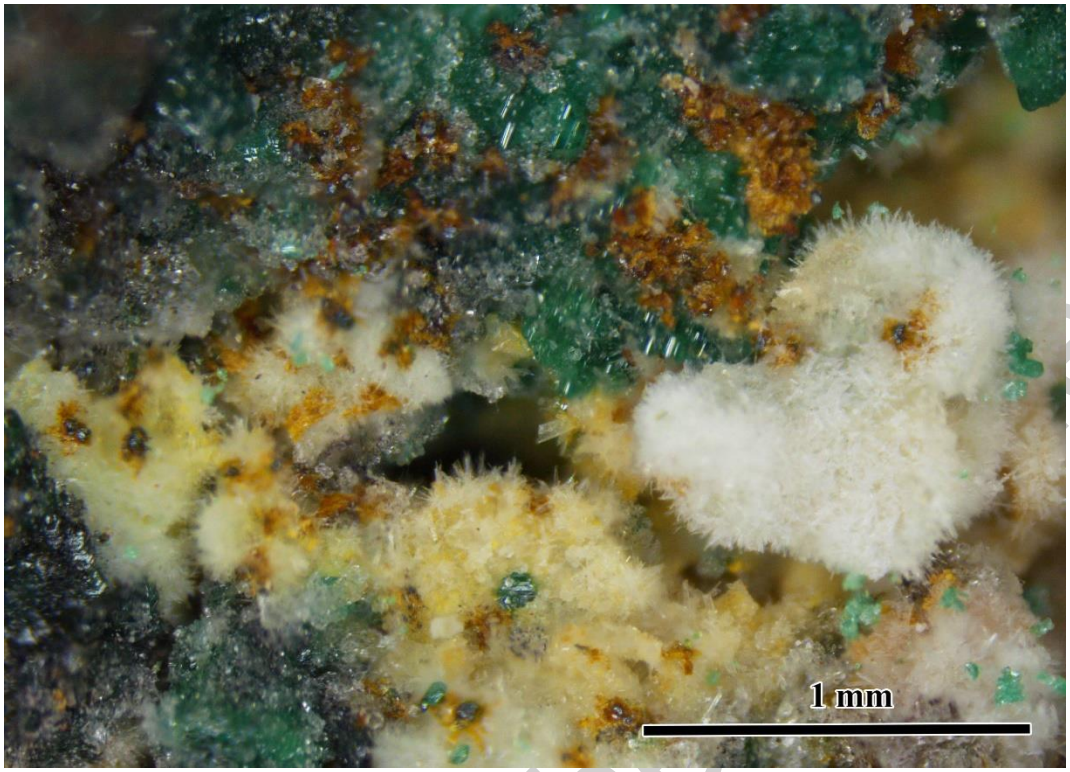

a

b

https://doi.org/10.1180/mgm.2025.10141 Published online by Cambridge University Press

Figure 2. Brown to brown-yellow aggregates of magganasite which overgrow green lammerite crystals (a, b) and white to yellowish sanidine crystal crusts (a). Black mineral is hematite and colourless transparent mineral forming small equant crystals is langbeinite.

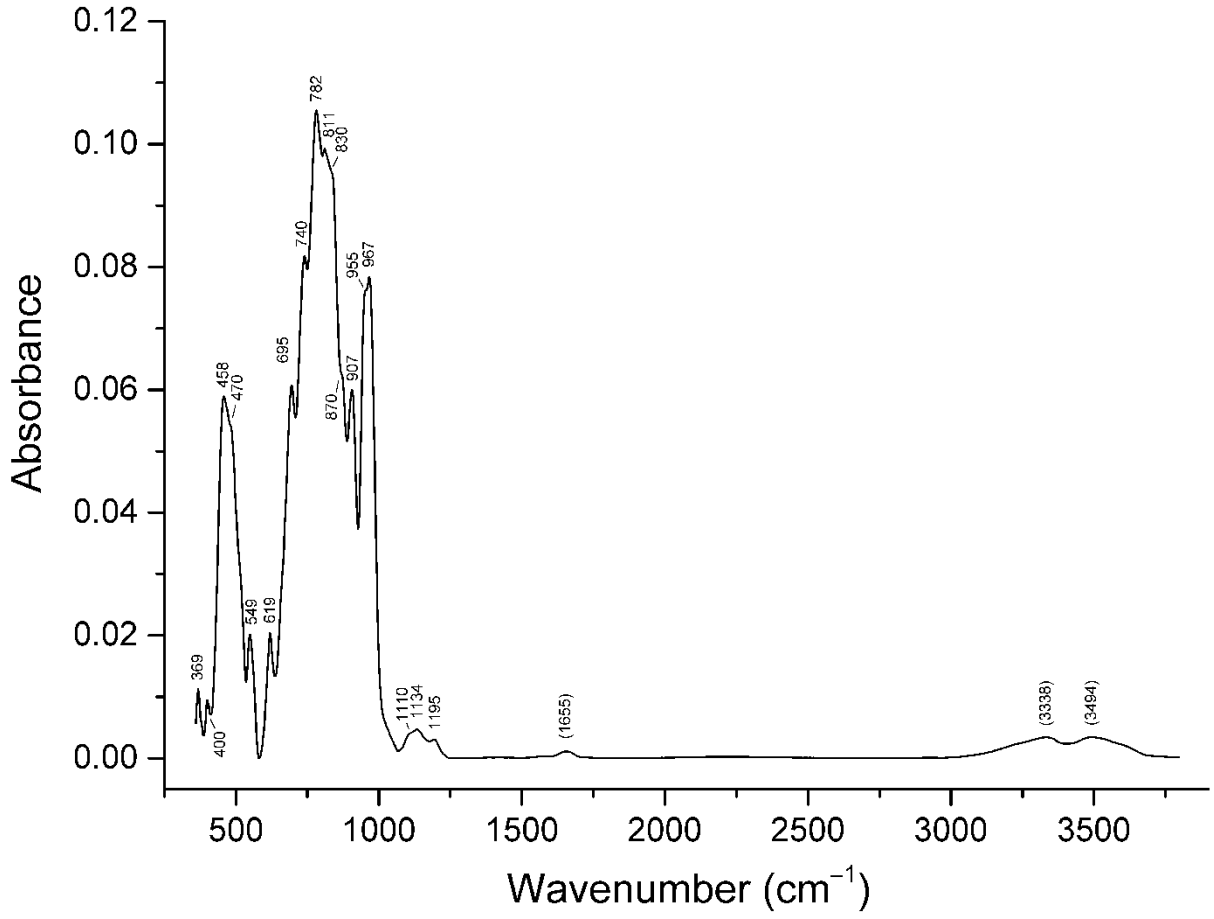

Figure 3. IR spectrum of magganasite. Wavenumbers of bands corresponding to water present in the sample (see text) are given in parentheses.

https://doi.org/10.1180/mgm.2025.10141 Published online by Cambridge University Press

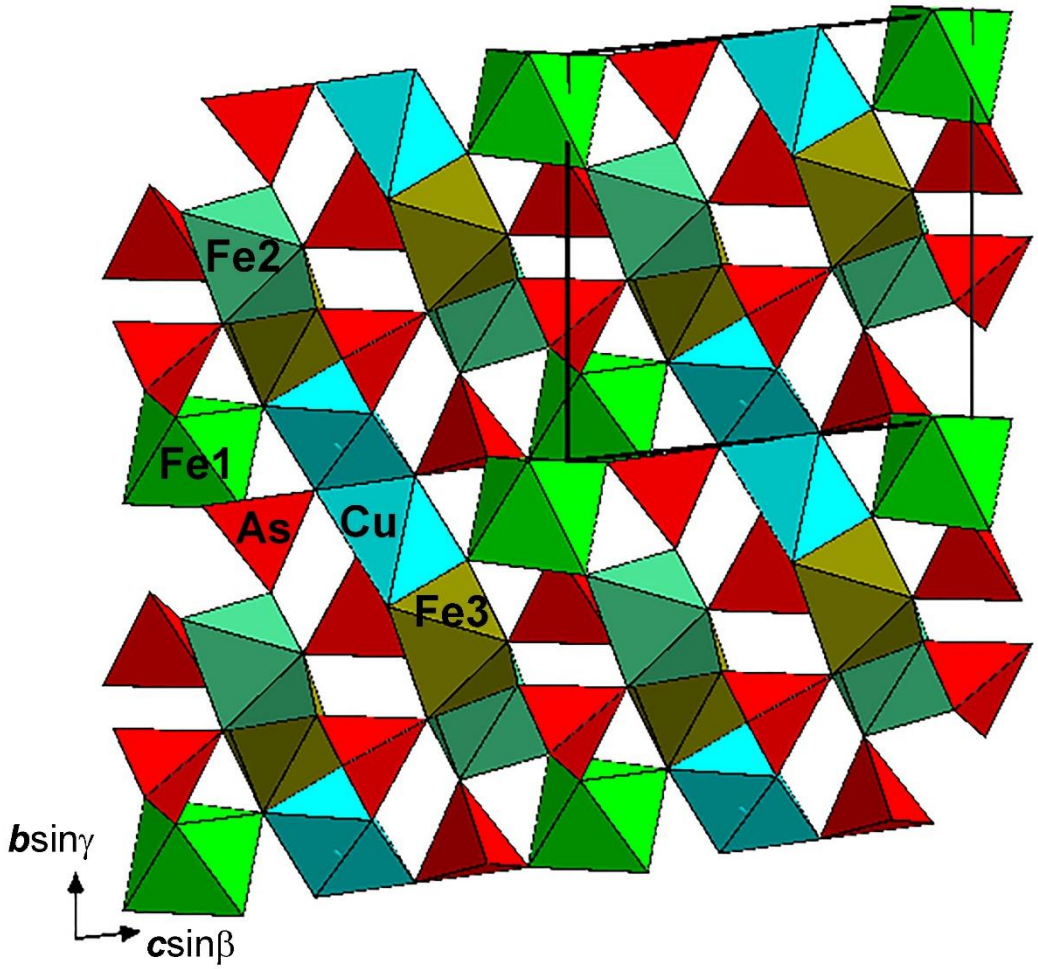

Figure 4. The crystal structure of magganasite projected along the *a* axis. The unit cell is outlined.

https://doi.org/10.1180/mgm.2025.10141 Published online by Cambridge University Press

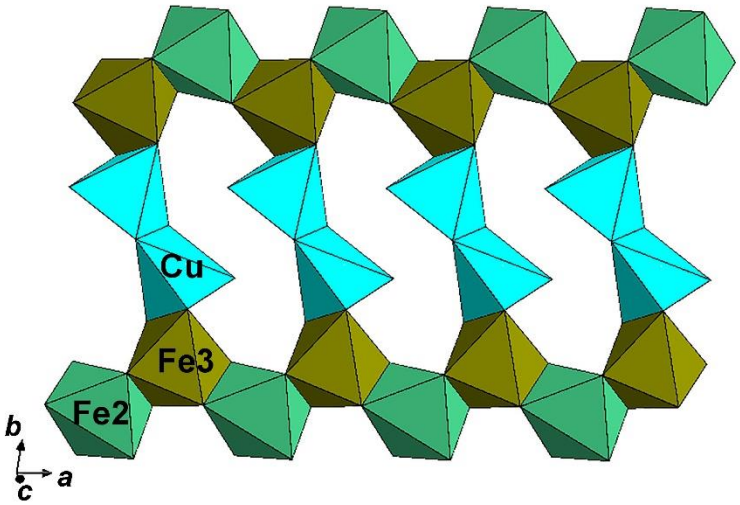

a

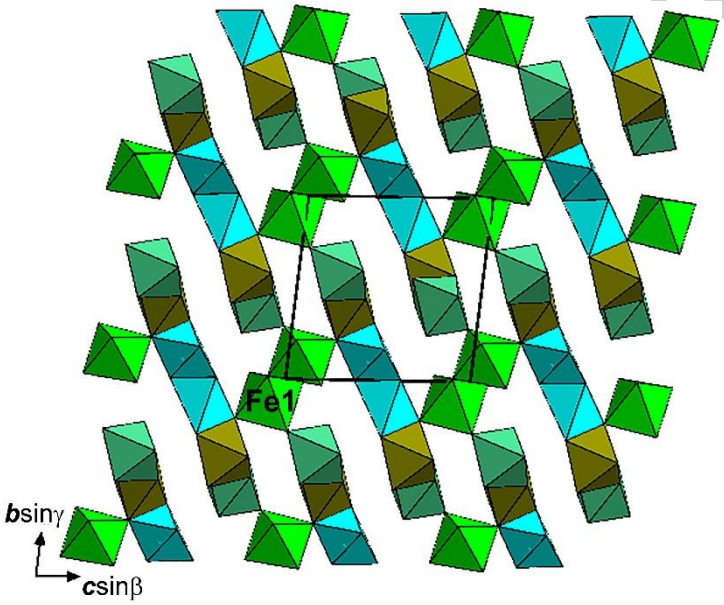

b

Figure 5. The ribbon built by Fe^{3+}-centred octahedra and Cu^{2+}-centred tetragonal pyramids (a) and the pseudo-framework built from *Me*-centred (*Me* = Fe, Cu) polyhedra (b) in the structure of magganasite.

https://doi.org/10.1180/mgm.2025.10141 Published online by Cambridge University Press